



Published in final edited form as:

*Science*. 2016 April 29; 352(6285): 595–599. doi:10.1126/science.aad9964.

## Phase separation of signaling molecules promotes T cell receptor signal transduction

Xiaolei Su<sup>1,2,\*</sup>, Jonathon A. Ditlev<sup>1,3,\*</sup>, Enfu Hui<sup>1,2</sup>, Wenmin Xing<sup>1,3</sup>, Sudeep Banjade<sup>1,3</sup>, Julia Okrut<sup>1,2</sup>, David S. King<sup>4</sup>, Jack Taunton<sup>1,2</sup>, Michael K. Rosen<sup>1,3</sup>, and Ronald D. Vale<sup>1,2</sup>

Michael K. Rosen: michael.rosen@utsouthwestern.edu; Ronald D. Vale: ron.vale@ucsf.edu

<sup>1</sup>The HHMI Summer Institute, Marine Biological Laboratory, Woods Hole, MA 02543, USA

<sup>2</sup>Department of Cellular and Molecular Pharmacology and Howard Hughes Medical Institute, University of California, San Francisco, CA 94158, USA

<sup>3</sup>Department of Biophysics and Howard Hughes Medical Institute, University of Texas Southwestern Medical Center, Dallas, TX 75390, USA

<sup>4</sup>Howard Hughes Medical Institute Mass Spectrometry Laboratory and Department of Molecular and Cellular Biology, University of California, Berkeley, CA 94720, USA

### Abstract

Activation of various cell surface receptors triggers the reorganization of downstream signaling molecules into micron- or submicron-sized clusters. However, the functional consequences of such clustering has been unclear. We biochemically reconstituted a 12-component signaling pathway on model membranes, beginning with T cell receptor (TCR) activation and ending with actin assembly. When TCR phosphorylation was triggered, downstream signaling proteins spontaneously separated into liquid-like clusters that promoted signaling outputs both in vitro and in human Jurkat T cells. Reconstituted clusters were enriched in kinases but excluded phosphatases, and enhanced actin filament assembly by recruiting and organizing actin regulators. These results demonstrate that protein phase separation can create a distinct physical and biochemical compartment that facilitates signaling.

### One Sentence Summary

Reconstitution of a T cell signaling pathway and correlative cellular studies reveal how phase separation of molecules into microclusters can promote biochemical reactions and signaling responses.

---

Correspondence to: Michael K. Rosen, michael.rosen@utsouthwestern.edu; Ronald D. Vale, ron.vale@ucsf.edu.

\*These authors contributed equally to this work.

### Supplementary Materials

[www.sciencemag.org](http://www.sciencemag.org)

Materials and Methods

Figures S1–S11

Table S1–S2

Movies S1–S5

Author contributions

References (28–32)

Many cell surface receptors and downstream signaling molecules coalesce into micron- or submicron-sized clusters upon initiation of signaling (<sup>1, 2</sup>). However, the effect of this clustering on signal transduction is poorly understood. T cell receptor (TCR) signaling is a well-studied example of this general phenomenon (<sup>3</sup>). TCR signaling proceeds through a series of biochemical reactions that can be viewed as connected modules. In the upstream module, the TCR is phosphorylated by Lck, a membrane-bound protein kinase of the Src family. TCR phosphorylation is opposed by a transmembrane phosphatase, CD45 (<sup>3</sup>). The phosphorylated cytoplasmic domains of the TCR complex recruit and activate the cytosolic tyrosine kinase ZAP70 (<sup>4</sup>). In the intermediate module, ZAP70 phosphorylates the transmembrane protein LAT (Linker for activation of T cells) on multiple tyrosine residues. These phosphotyrosines are binding sites for adapter proteins Grb2 and Gads, which further interact with Sos1 (a guanine nucleotide exchange factor (GEF) for the small guanosine triphosphatase Ras) or SLP-76 (another adaptor in TCR signaling). Components of the LAT complex activate several downstream modules that mediate calcium mobilization, mitogen-activated protein kinase (MAPK) activation, and actin polymerization (<sup>5, 6</sup>).

LAT and its binding partners coalesce into micron- or submicron-sized clusters at the plasma membrane upon TCR activation (<sup>7–10</sup>). Elimination of these microclusters by deletion of key components (for example, LAT or Grb2) impairs downstream signaling and transcriptional responses (<sup>5, 11</sup>). However, effects due to loss of clusters have not been distinguished from those due to loss of component molecules. Nor do we understand the changes in biochemistry and consequent signaling that emerge specifically when signaling molecules are organized from an unclustered to a clustered state (<sup>12</sup>).

To explore the mechanism of formation and functional consequences of T cell microclusters, we reconstituted a TCR signaling pathway from purified components. To substitute for the plasma membrane, we used supported bilayers composed of a defined, simple lipid composition. We initially reconstituted the intermediate module of the TCR signaling cascade, composed of phosphorylated LAT (pLAT), Grb2, and Sos1. Multivalent interactions between these proteins (Fig. 1A) are thought to drive the formation of signaling microclusters on the T cell membrane (<sup>8, 13</sup>), although direct experimental evidence for the sufficiency of this mechanism has been lacking. We prepared fluorescently labeled pLAT, containing the four C-terminal phospho-tyrosine residues that are sufficient for TCR signaling (<sup>14</sup>); this pLAT also contains an N-terminal His<sub>8</sub> tag that allowed its attachment to Ni<sup>2+</sup>-containing supported lipid bilayers (<sup>15</sup>). pLAT was uniformly distributed (Fig. 1B) and freely diffused on the lipid bilayer (movie S1). Upon addition of Grb2 and Sos1, submicron-sized clusters formed within 1 minute and gradually grew in size. Cluster formation required tyrosine phosphorylation of LAT (fig. S1D). Furthermore, dephosphorylation of pLAT by high concentrations of the soluble protein tyrosine phosphatase 1B (PTP1B, 2 μM) caused the clusters to disassemble (Fig. 1B, movie S2). pLAT, Grb2, and Sos1 all colocalized within clusters, and clusters did not form if either Grb2 or Sos1 was omitted (fig. S1E, F). pLAT also clustered with Gads and SLP-76, two other components of LAT clusters in cells (<sup>6, 7</sup>), but less efficiently than with Grb2 and Sos1 (fig. S2A, B). Clustering efficiency, however, increased dramatically with the addition of Nck (fig. S2C), an adaptor protein known to link SLP-76 to actin regulators (<sup>16</sup>).

pLAT, Grb2, and Sos1 clusters exhibited dynamic liquid-like properties. The rounded edges of clusters fluctuated (extending and retracting) on a time scale of seconds and clusters sometimes fused with one another (movie S2). pLAT molecules exchanged into and out of clusters, as revealed by fluorescence recovery after photobleaching (FRAP) (Fig. 1C). Single pLAT molecules diffused rapidly outside of clusters but slowly within them (fig. S3A–C). We also observed capture and release of single molecules by clusters (movie S3). These results show that pLAT microclusters are liquid-like, phase-separated structures (17, 18) on membranes.

Both SH3 domains of Grb2 were required for cluster formation, indicating a role of protein cross-bridging by this adaptor protein (Fig. 1D and fig. S4A). Clustering initially increased with increasing pLAT density but then decreased at higher pLAT densities on the membrane (fig. S4B), consistent with a theoretical multivalent interaction model (19). The valency of phospho-tyrosines on LAT also affected clustering efficiency. Three of the four distal phospho-tyrosines in LAT are recognized by the SH2 domain of Grb2 (20). Clustering in vitro progressively decreased by mutating one, two, or all three tyrosines and was enhanced by doubling the number of tyrosines (Fig. 1E and fig. S5). Together, our data indicate that LAT cluster formation is driven by dynamically rearranging, multivalent protein-protein interactions.

We compared the properties of LAT clusters in cells with those of reconstituted clusters in vitro and tested their functional importance. As in vitro, LAT microclusters in T cells sometimes fused with one another (fig. S3D). FRAP revealed that molecules exchange into and out of clusters in cells faster than in vitro ( $t_{1/2}$  of 12 sec versus 76 sec), possibly due to different cluster size (see Supplementary Text) or membrane fluidity. To assess valency dependence in cells, we expressed LAT tyrosine mutants with zero, one, two, three, or six Grb2 binding sites in a LAT-deficient Jurkat T cell line. A minimum of two Grb2 binding sites was required for robust cluster formation and the degree of clustering increased with increasing number of phospho-tyrosine sites (Fig. 2B). The degree of clustering correlated with activation of MAPK(ERK) (Fig. 2C), suggesting that clustering of LAT and its partners is important for TCR signaling.

We used our in vitro assay to gain insight into the biochemical reactions that underlie the TCR signaling pathway. To LAT and its binding partners, we introduced the upstream signaling module consisting of: i) the cytoplasmic domain of the TCR subunit CD3 $\zeta$  (which is sufficient to induce signaling in T cells (21)), ii) Lck, which phosphorylates the TCR, iii) the cytoplasmic domain of the tyrosine phosphatase CD45, which opposes this reaction (22), and iv) the protein kinase ZAP70, which is recruited to the phosphorylated TCR and phosphorylates LAT (4, 5) (Fig. 3A). Initially, unphosphorylated LAT was evenly distributed on the membrane. After ATP was added to initiate Lck phosphorylation of CD3 $\zeta$ , ZAP70 was recruited to the membrane and LAT clustered (Fig. 3B; fig. S6A). ZAP70 was enriched in the clusters, as observed in T cells (7), whereas CD45 was excluded (Fig. 3B). The exclusion of CD45 was recapitulated in a simpler system in which clusters were formed by pLAT, Grb2, and Sos1 (Fig. 3C). The cytoplasmic domain of CD45 has a negative charge (pI 6.4). Assays with a series of differentially charged proteins revealed that, in general, positive charge favors inclusion into and negative charge favors exclusion from LAT clusters (fig. S7

and Supplementary Text). Consistent with limited access of CD45 to pLAT in the cluster center, CD45-mediated dephosphorylation of pLAT was reduced compared to that in unclustered conditions (Fig. 3D). In summary, our data demonstrate that LAT clusters are depleted in the phosphatase CD45 but enriched in the kinase ZAP70, which would be expected to promote LAT phosphorylation and increase the strength of TCR signaling.

We sought to integrate a downstream module that controls an important signaling output, actin polymerization (23, 24). We attached His-tagged Lck, CD3 $\zeta$ , and unphosphorylated LAT-Alexa647 to the supported lipid bilayer and added soluble ZAP70-505-Star, Gads, SLP-76, Nck, N-WASp (neuronal Wiskott-Aldrich Syndrome protein), Arp2/3 (Actin-related protein 2 and 3) complex, and rhodamine-labeled monomeric actin to the solution (Fig. 4A). Previous data have shown that Nck recruits N-WASp, which in turn activates the Arp2/3 complex to nucleate actin filaments (16, 25). When ATP was added to initiate TCR phosphorylation, ZAP70 was recruited to the membrane, followed by LAT clustering and then actin polymerization from the LAT clusters (Fig. 4B,C and fig. S8). Later, when actin bundles formed, LAT clusters became rod-like and aligned with actin bundles (Fig. 4D and movie S4,5). This shape change is reversible, as clusters became round following depolymerization of F-actin by Latrunculin A (fig. S9C). In summary, we show that actin polymerization is initiated from and can reorganize LAT clusters.

We next tested if clustering of Nck affects the efficiency of actin polymerization. In principle, actin polymerization could be stimulated by i) recruitment of Nck from solution to the membrane, ii) concentration and organization of Nck within clusters, or iii) both effects. To isolate spatial distribution as a variable, we attached His<sub>10</sub>-Nck to Ni-modified lipids in the planar bilayer, and added soluble N-WASp, Arp2/3 complex, and actin. Increasing the density of Nck on the membrane resulted in a dose-dependent increase in assembly of actin (fig. S10). Using a density of Nck (150 molecules/ $\mu\text{m}^2$ ) at which little actin polymerized, we tested whether clustering of Nck by pLAT, Gads, and pSLP-76 affected actin assembly. Clustering of Nck enhanced total actin assembly on the membrane by 6-fold (Fig. 4E). These results reveal that the clustering of actin regulators by LAT promotes actin polymerization beyond what can be achieved by recruitment to the membrane.

In summary, we reconstituted biochemical reactions of TCR signaling in an in vitro system, in which the components and their concentrations in the reaction can be controlled, rates can be measured, and molecular behaviors can be observed in ways that are difficult to achieve using intact cells. We observed multivalent assembly and consequent phase separation of LAT and its binding partners into liquid-like, micron-sized clusters. By manipulating clustering using LAT phosphorylation mutants, we show that clustering occurs through analogous mechanisms in vitro and in cells, and that clustering promotes MAPK(ERK) signaling. Thus, as in three-dimensional phase separation (17, 26), our results demonstrate that phase separation on membranes can create an environment that promotes biochemical reactions. LAT clusters excluded CD45 and retained ZAP70 to create an environment that perpetuated the phosphorylated state of LAT. Clustering of LAT promoted downstream biochemical reactions in the signaling pathway, specifically the ability of Nck to promote N-WASp-Arp2/3 mediated actin polymerization (fig. S11), as suggested by Nck density-dependent actin polymerization in cells (27). Multivalent interactions have been proposed to

drive the assembly of many other cellular structures, including PML bodies, stress granules, and focal adhesions (<sup>17, 26</sup>), thus the mechanisms of spatial organization of biochemical reactions revealed here may apply to other cellular processes as well.

## Supplementary Material

Refer to Web version on PubMed Central for supplementary material.

## Acknowledgments

We thank Steve Ross and Lynne Chang at Nikon Instruments for their loan of TIRF-capable microscopes, Nico Stuurman for help with microscopy, Art Weiss for providing JCam2.5 cells, David Liu for providing charged GFP constructs, Chi Pak for providing charged GFP proteins, James Muller for providing ICAM-1 protein, and Luke Rice, Xing Zeng, and members from the Vale Laboratory for comments on this manuscript. This work was supported by the HCIA program of HHMI, the NIH (R01-GM56322 to M.K.R.) and Welch Foundation (I-1544 to M.K.R.). X.S. was supported by CRI Irvington postdoctoral fellowship. J.A.D. was supported by NRSA F32 award 5-F32-DK101188. E.H. was supported as a fellow of the Leukemia and Lymphoma Society. J.O. was supported by funds from Tobacco-Related Disease Research Program of the University of California (19FT-0090).

## References and Notes

1. Wu H. Higher-order assemblies in a new paradigm of signal transduction. *Cell*. 2013; 153:287–292. [PubMed: 23582320]
2. Bienz M. Signalosome assembly by domains undergoing dynamic head-to-tail polymerization. *Trends in biochemical sciences*. 2014; 39:487–495. [PubMed: 25239056]
3. Chakraborty AK, Weiss A. Insights into the initiation of TCR signaling. *Nature immunology*. 2014; 15:798–807. [PubMed: 25137454]
4. Chan AC, Iwashima M, Turck CW, Weiss A. ZAP-70: a 70 kd protein-tyrosine kinase that associates with the TCR zeta chain. *Cell*. 1992; 71:649–662. [PubMed: 1423621]
5. Zhang W, Sloan-Lancaster J, Kitchen J, Tribble RP, Samelson LE. LAT: the ZAP-70 tyrosine kinase substrate that links T cell receptor to cellular activation. *Cell*. 1998; 92:83–92. [PubMed: 9489702]
6. Abraham RT, Weiss A. Jurkat T cells and development of the T-cell receptor signalling paradigm. *Nature reviews. Immunology*. 2004; 4:301–308.
7. Bunnell SC, Hong DI, Kardon JR, Yamazaki T, McGlade CJ, Barr VA, Samelson LE. T cell receptor ligation induces the formation of dynamically regulated signaling assemblies. *The Journal of cell biology*. 2002; 158:1263–1275. [PubMed: 12356870]
8. Douglass AD, Vale RD. Single-molecule microscopy reveals plasma membrane microdomains created by protein-protein networks that exclude or trap signaling molecules in T cells. *Cell*. 2005; 121:937–950. [PubMed: 15960980]
9. Varma R, Campi G, Yokosuka T, Saito T, Dustin ML. T cell receptor-proximal signals are sustained in peripheral microclusters and terminated in the central supramolecular activation cluster. *Immunity*. 2006; 25:117–127. [PubMed: 16860761]
10. Singleton KL, Roybal KT, Sun Y, Fu G, Gascoigne NR, van Oers NS, Wulfing C. Spatiotemporal patterning during T cell activation is highly diverse. *Science signaling*. 2009; 2:ra15. [PubMed: 19351954]
11. Bilal MY, Houtman JC. GRB2 Nucleates T Cell Receptor-Mediated LAT Clusters That Control PLC-gamma1 Activation and Cytokine Production. *Frontiers in immunology*. 2015; 6:141. [PubMed: 25870599]
12. Dustin ML, Groves JT. Receptor signaling clusters in the immune synapse. *Annual review of biophysics*. 2012; 41:543–556.
13. Houtman JC, Yamaguchi H, Barda-Saad M, Braiman A, Bowden B, Appella E, Schuck P, Samelson LE. Oligomerization of signaling complexes by the multipoint binding of GRB2 to both LAT and SOS1. *Nature structural & molecular biology*. 2006; 13:798–805.

14. Zhu M, Janssen E, Zhang W. Minimal requirement of tyrosine residues of linker for activation of T cells in TCR signaling and thymocyte development. *Journal of immunology*. 2003; 170:325–333.
15. Materials and methods are available as supplementary materials on Science Online.
16. Wunderlich L, Farago A, Downward J, Buday L. Association of Nck with tyrosine-phosphorylated SLP-76 in activated T lymphocytes. *European journal of immunology*. 1999; 29:1068–1075. [PubMed: 10229072]
17. Li P, Banjade S, Cheng HC, Kim S, Chen B, Guo L, Llaguno M, Hollingsworth JV, King DS, Banani SF, Russo PS, Jiang QX, Nixon BT, Rosen MK. Phase transitions in the assembly of multivalent signalling proteins. *Nature*. 2012; 483:336–340. [PubMed: 22398450]
18. Banjade S, Rosen MK. Phase transitions of multivalent proteins can promote clustering of membrane receptors. *eLife*. 2014; 3
19. Nag A, Monine MI, Faeder JR, Goldstein B. Aggregation of membrane proteins by cytosolic cross-linkers: theory and simulation of the LAT-Grb2-SOS1 system. *Biophysical journal*. 2009; 96:2604–2623. [PubMed: 19348745]
20. Tinti M, Kiemer L, Costa S, Miller ML, Sacco F, Olsen JV, Carducci M, Paoluzi S, Langone F, Workman CT, Blom N, Machida K, Thompson CM, Schutkowski M, Brunak S, Mann M, Mayer BJ, Castagnoli L, Cesareni G. The SH2 domain interaction landscape. *Cell reports*. 2013; 3:1293–1305. [PubMed: 23545499]
21. Irving BA, Weiss A. The cytoplasmic domain of the T cell receptor zeta chain is sufficient to couple to receptor-associated signal transduction pathways. *Cell*. 1991; 64:891–901. [PubMed: 1705867]
22. Hui E, Vale RD. In vitro membrane reconstitution of the T-cell receptor proximal signaling network. *Nature structural & molecular biology*. 2014; 21:133–142.
23. Kumari S, Depoil D, Martinelli R, Judokusumo E, Carmona G, Gertler FB, Kam LC, Carman CV, Burkhardt JK, Irvine DJ, Dustin ML. Actin foci facilitate activation of the phospholipase C-gamma in primary T lymphocytes via the WASP pathway. *eLife*. 2015; 4
24. Bunnell SC, Kapoor V, Tribble RP, Zhang W, Samelson LE. Dynamic actin polymerization drives T cell receptor-induced spreading: a role for the signal transduction adaptor LAT. *Immunity*. 2001; 14:315–329. [PubMed: 11290340]
25. Rohatgi R, Nollau P, Ho HY, Kirschner MW, Mayer BJ. Nck and phosphatidylinositol 4,5-bisphosphate synergistically activate actin polymerization through the N-WASP-Arp2/3 pathway. *The Journal of biological chemistry*. 2001; 276:26448–26452. [PubMed: 11340081]
26. Hyman AA, Weber CA, Julicher F. Liquid-liquid phase separation in biology. *Annual review of cell and developmental biology*. 2014; 30:39–58.
27. Ditlev JA, Michalski PJ, Huber G, Rivera GM, Mohler WA, Loew LM, Mayer BJ. Stoichiometry of Nck-dependent actin polymerization in living cells. *The Journal of cell biology*. 2012; 197:643–658. [PubMed: 22613834]

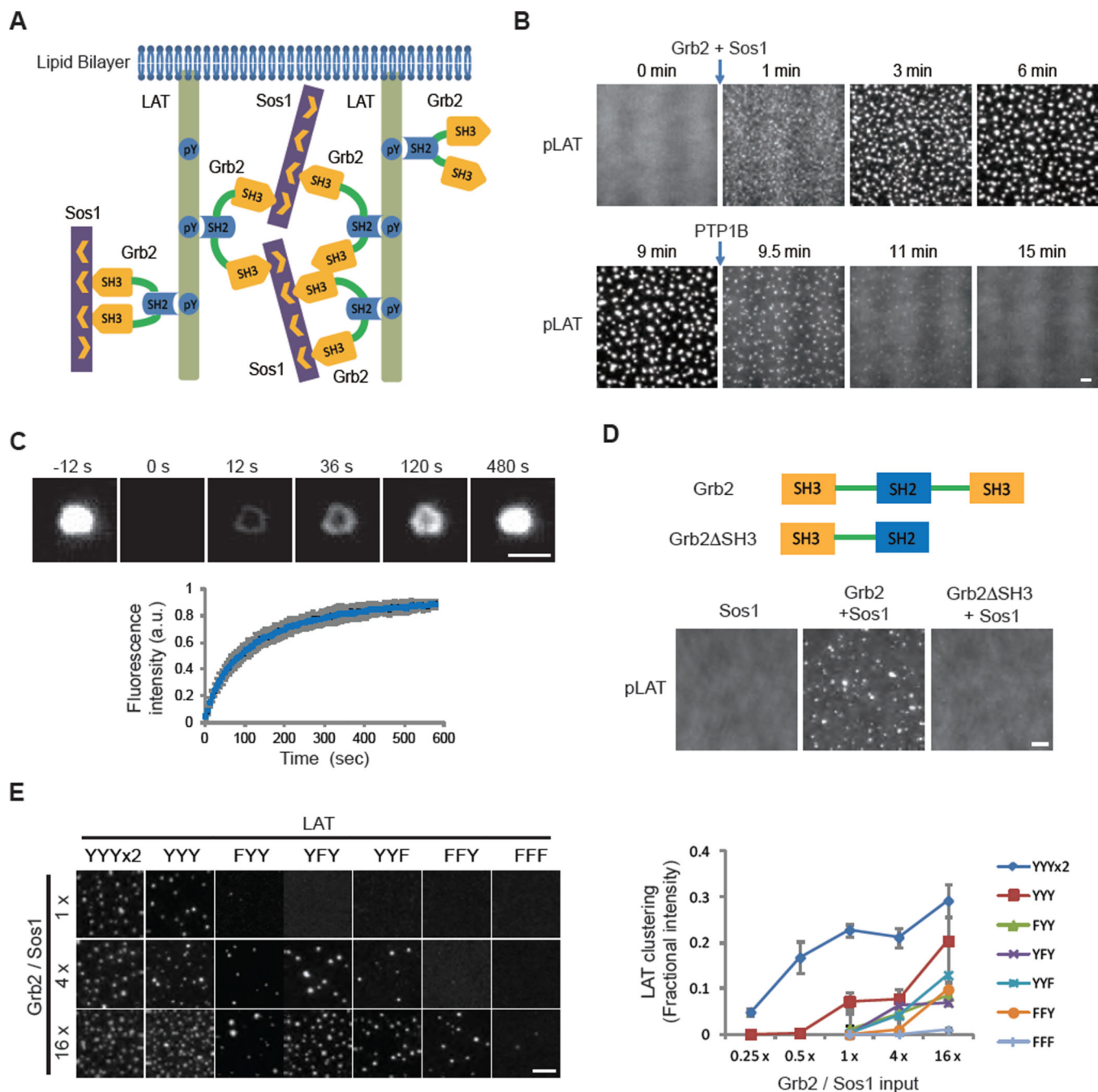


**Fig. 1. Multivalent interactions drive LAT cluster formation**

(A) Schematic of the proteins and interactions in the clustering assay. (B) Total internal reflection fluorescence microscopy (TIRF) imaging of LAT clustering and de-clustering. Clusters formed after adding Grb2 (0.5  $\mu\text{M}$ ) and Sos1 (0.25  $\mu\text{M}$ , the proline-rich motifs) to membrane-bound pLAT-Alexa488 (1000 molecules/ $\mu\text{m}^2$ ) at 0 min and dissolved after adding the protein tyrosine phosphatase PTP1B (2  $\mu\text{M}$ ) at 9 min. Scale bar: 2  $\mu\text{m}$ . See movie S2. (C) Fluorescence recovery after photobleaching (FRAP) of clustered pLAT on planar lipid bilayers; time 0 indicates the time of the photobleaching pulse. Bottom plot shows the time course of the recovery of pLAT-Alexa488 (300 molecules/ $\mu\text{m}^2$ ) formed by 1  $\mu\text{M}$  Grb2

and 2  $\mu\text{M}$  Sos1. Shown are the mean  $\pm$  s.d. (N=7 pLAT clusters). Scale bar, 2  $\mu\text{m}$ . **(D)** TIRF imaging of pLAT-Alexa488 (300 molecules/ $\mu\text{m}^2$ ) with Sos1 (0.5  $\mu\text{M}$ ) alone or additionally with wild-type Grb2 (0.5  $\mu\text{M}$ ) or Grb2 SH3 (1  $\mu\text{M}$ ) (note-concentrations were set to maintain identical total SH3 concentrations in the experiments containing Grb2 and Grb2 SH3). Scale bar: 2  $\mu\text{m}$ . **(E)** Valency-dependent clustering of pLAT. **LEFT:** pLAT wild-type with three Grb2 phosphorylation sites (YYY) or mutants that contain 6 (2xYYY), 2 (FYY, YFY, YFF), 1 (FFY), or 0 (FFF) phospho-tyrosines were incubated with increasing concentrations of Grb2 and Sos1. 1x indicates 125 nM Grb2 and 62 nM Sos1. pLAT valency mutants were plated at a density around 300 molecules/ $\mu\text{m}^2$ . Clusters were imaged by TIRF microscopy. Scale bar: 5  $\mu\text{m}$ . **RIGHT:** Quantification of clustering of pLAT valency mutants. Clustering degree was quantified by fractional intensity. Phase diagrams of pLAT mutants using a larger range of Grb2 and Sos1 concentrations are shown in fig. S5. Values shown are the mean  $\pm$  s.d. (N=3 independent experiments).



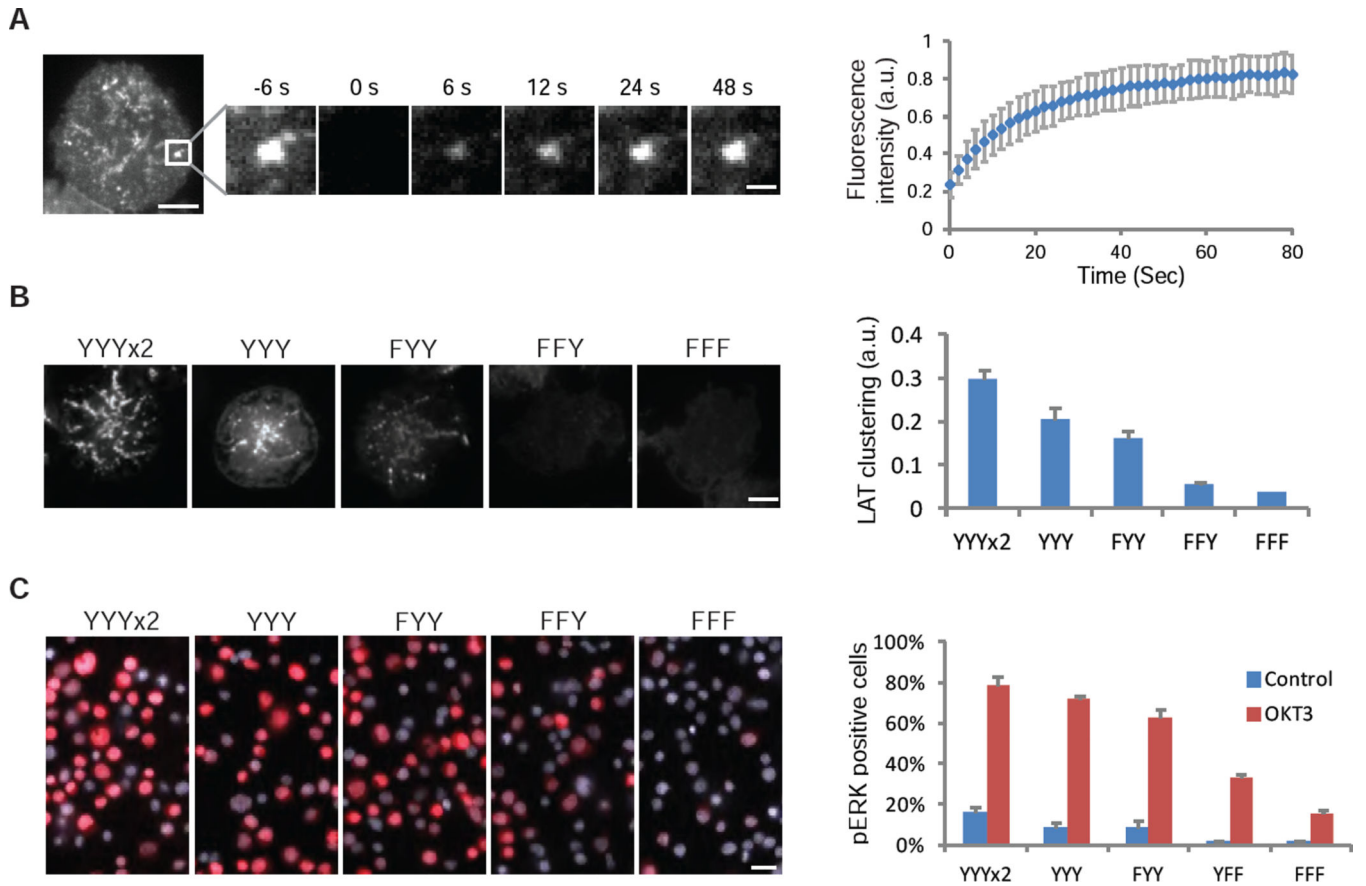


**Fig. 2. LAT clustering promotes MAPK(ERK) signaling in T cells**

(A) Fluorescence recovery after photobleaching (FRAP) of LAT-mCitrine clusters on plasma membranes of Jurkat T cells activated by anti-CD3 antibody (OKT3 at 5  $\mu\text{g}/\text{mL}$ ) attached to the coverslip; time 0 indicates the time of the photobleaching pulse. Scale bar, 5  $\mu\text{m}$  or 1  $\mu\text{m}$  on the enlarged panel. Right plot shows the time course of the recovery (mean  $\pm$  s.d.) of 15 cells. (B) TIRF microscopy revealed cluster formation of LAT variants in activated T cells. A LAT-deficient line (Jcam2.5) stably expressing LAT variants containing 6 (2x YYY), 3 (YYY), 2 (FYY), 1 (FFY), or 0 (FFF) tyrosines for Grb2 binding, was activated by plate-presented OKT3 at 5  $\mu\text{g}/\text{mL}$ . See Methods for clustering quantification. Scale Bar: 5  $\mu\text{m}$ . Shown are mean  $\pm$  s.e.m. (N=16–20 cells). (C) MAPK(ERK) activation in Jurkat T cells expressing LAT valency mutants. Cells were activated by anti-CD3 antibody OKT3 at 5  $\mu\text{g}/\text{mL}$ , fixed at 10 min, and stained with an antibody to pERK (red) and a nucleus dye Hoechst (blue). Scale bar, 20  $\mu\text{m}$ . Right plot shows the percentage of pERK positive cells. 200–300 cells were scored for each data point. Shown are mean  $\pm$  s.e.m. (N=3 independent experiments).

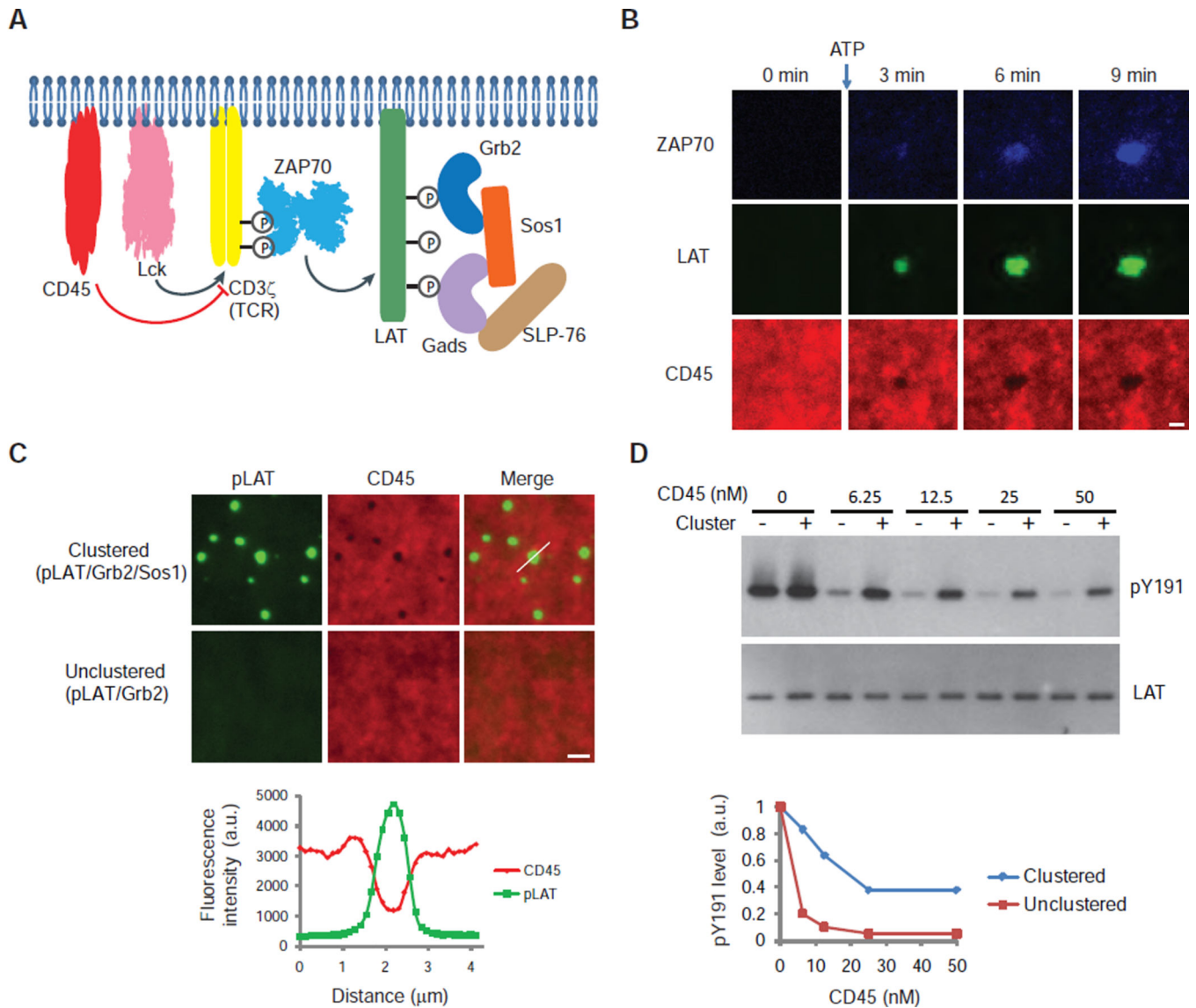


**Fig. 3. Reconstitution of TCR phosphorylation to LAT clustering**

(A) Schematic of components in a reaction designed to reconstitute signaling from TCR/CD3 $\zeta$  phosphorylation to LAT clustering. The cytoplasmic domains of CD45, Lck, CD3 $\zeta$ , and LAT were polyhistidine-tagged for membrane attachment and incubated with other components in solution. ATP was added to trigger the phosphorylation cascade. Input: CD45-SNAP-TMR, Lck, CD3 $\zeta$ , and LAT-Alexa647 at 30, 250, 500, and 1000 molecules/ $\mu\text{m}^2$  respectively, 10 nM ZAP70-505-Star, 250 nM Grb2, 125 nM Sos1, 250 nM Gads, 125 nM SLP-76, and 0.5 mM ATP-Mg. (B) TIRF microscopy revealed time courses of ZAP70 membrane recruitment, CD45 exclusion, and LAT clustering in the reconstituted pathway. A larger field view of LAT clusters is shown in fig. S6B. Scale bar: 2  $\mu\text{m}$ . (C) TOP: pLAT-Alexa488 (300 molecules/ $\mu\text{m}^2$ ) bound to planar lipid bilayers was incubated with Grb2 (1  $\mu\text{M}$ ) in the presence (top) or absence (bottom) of Sos1 (1  $\mu\text{M}$ ). Then the cytoplasmic domain of CD45-TMR (4 nM; with an N-terminal His<sub>10</sub> tag) was added and its localization was visualized by TIRF microscopy. Scale bar: 2  $\mu\text{m}$ . BOTTOM: Quantification of fluorescence

intensity of pLAT and CD45 along the line scan indicated by a white line in the top merged image. **(D)** Western blot analysis of pLAT dephosphorylation by CD45. pLAT bound to membrane (300 molecules/ $\mu\text{m}^2$ ) was incubated with 1  $\mu\text{M}$  Grb2 (unclustered pLAT) or 1  $\mu\text{M}$  Grb2 plus 1  $\mu\text{M}$  Sos1 (clustered pLAT). His<sub>10</sub>-CD45 was then added and the reactions were stopped after 5 min by adding SDS-PAGE loading buffer containing 2 mM vanadate. Quantification of pLAT phosphorylation normalized to the total LAT signal is shown in the bottom plot.

Author Manuscript

Author Manuscript

Author Manuscript

Author Manuscript

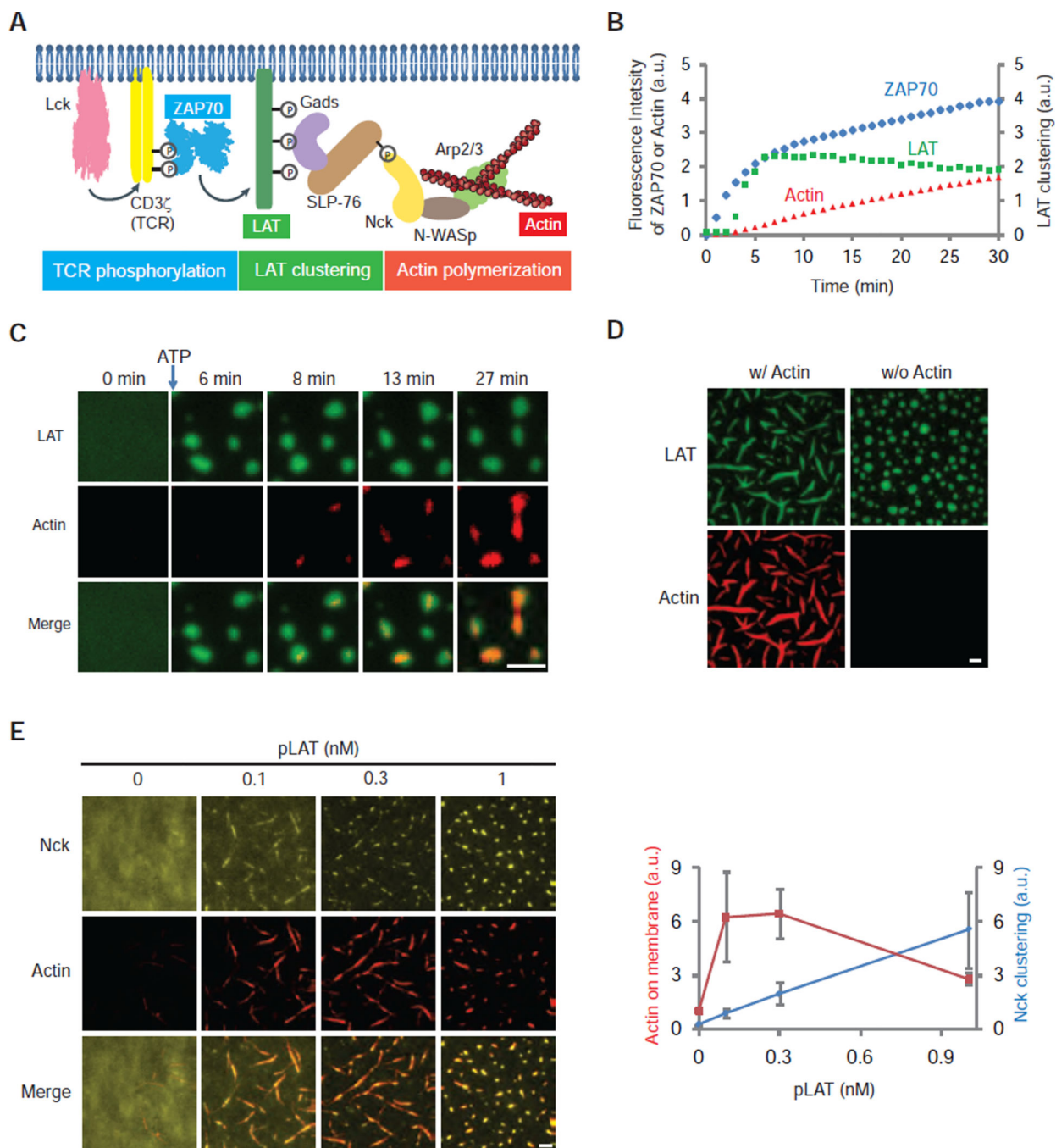


**Fig. 4. LAT clustering promotes actin polymerization**

(A) Schematic of the reconstituted signaling pathway from CD3 $\zeta$ /TCR phosphorylation to actin polymerization. ZAP70-505-Star, LAT-Alexa647, and actin-Rhodamine serve as reporters for TCR phosphorylation, LAT clustering, and actin assembly, respectively. Lck, CD3 $\zeta$ , and LAT were membrane attached through a polyhistidine tag and incubated with other components in solution. ATP was then added to trigger the signaling cascade. Input: same for Lck, CD3 $\zeta$ , pLAT-Alexa647, and ZAP70-505-Star as described in Fig. 3A. The rest are 250 nM Gads, 125 nM SLP-76, 500 nM Nck, 250 nM N-WASp, 2.5 nM Arp2/3

complex, 500 nM actin (5% Rhodamine labeled), and 0.5 mM ATP-Mg. **(B)** Time courses of ZAP70 membrane recruitment, LAT clustering, and actin polymerization in the reconstituted assay after addition of ATP at time 0. LAT clustering was quantified as variance of fluorescence intensities on membranes (See Methods). **(C)** TIRF imaging showing actin assembly on the LAT clusters. Scale bar: 2  $\mu\text{m}$ . **(D)** TIRF imaging of pLAT-Alexa647 and actin-Rhodamine 45 min after adding ATP to the reaction. Input: same as in Fig. 4A except with higher concentrations of components of actin and actin regulators (500 nM SLP-76, 1000 nM Nck, 500 nM N-WASp, 5 nM Arp2/3 complex, 1000 nM actin (5% Rhodamine-labeled)). Scale bar: 2  $\mu\text{m}$ . **(E)** LEFT: TIRF microscopy images of His<sub>10</sub>-Nck-Pacific Blue and actin-Rhodamine on the bilayer. Nck (150 molecules/ $\mu\text{m}^2$ ) was attached to the bilayer and N-WASp (5 nM), Arp2/3 complex (0.25 nM), actin (200 nM; 5% Rhodamine labeled), and 0.5 mM ATP-Mg were in solution. Increasing concentrations of His-tagged pLAT were added as indicated along with Gads and pSLP-76. At 0.1 nM pLAT, Gads, and pSLP-76 concentrations were 8 nM and 4 nM, respectively. As pLAT concentration was increased, more Gads and pSLP-76 were added to maintain a constant ratio of the clustering components. Scale bar: 2  $\mu\text{m}$ . RIGHT: Mean actin fluorescence (red) and Nck clustering level (blue) quantified as variance of His<sub>10</sub>-Nck fluorescence intensity, are plotted for increasing concentrations of pLAT. Shown are mean  $\pm$  s.e.m. (N=3 independent experiments).